ELSEVIER

Effective parameters of the band dispersion in n-type high-T_c superconductors

M.M. Korshunov [a], V.A. Gavrichkov [a], S.G. Ovchinnikov [a],
D. Manske [b], I. Eremin [b,*]

[a] *L.V. Kirensky Institute of Physics, Siberian Branch of Russian Academy of Science, Krasnoyarsk 660036, Russia*
[b] *Institut für Theoretische Physik, Freie Universität Berlin, Arnimallee 14, D-14195 Berlin, Germany*

Abstract

The electronic structure of electron-doped cuprates is discussed in the regions of small and optimal doping. For optimal doping we obtain the parameters from a simple tight-binding analysis by fitting ARPES data, and for small doping we study the band structure by the generalized tight-binding method that takes strong electronic correlations into account explicitly. This method has also reproduced well the ARPES data for small doping. The effective low-energy Hamiltonian is the t–t'–J model with hopping parameters t and t'. We compare both methods and find very good agreement for the value of t while t' is different because it is caused by the different contribution of the short-range spin correlations.
© 2003 Elsevier B.V. All rights reserved.

It is widely believed that it is impossible to formulate a complete theory of high-T_c superconductivity (HTSC) in cuprates without understanding the behavior not only of the hole doped HTSC (p-type cuprates: LSCO, YBCO, Bi2212, etc.), but also electron doped systems (n-type cuprates: NCCO, PCCO). While having similar structure of CuO_2 layers these compounds have different electronic properties. Most intriguing examples of these properties are: (i) the phase diagram [1] is asymmetric for p- and n-type systems, (ii) the resistivity in the normal state of NCCO is described by a Fermi liquid square-law dependence on temperature [2] in contrast to the linear dependence in p-type HTSC [3], (iii) the insulating gap in n-type systems is indirect [4] (the minimum of conduction band and maximum of a valence band are in different points of Brillouin zone), (iv) in contrast to LSCO where pinning of the chemical potential takes place at small x, doping dependence of the chemical potential in NCCO is more complex [5].

The origin of this asymmetry of the electronic properties should lie in different crystal structure

* Corresponding author. Tel.: +49-30-8385-1422; fax: +49-30-8385-7422.
E-mail address: ieremin@physik.fu-berlin.de (I. Eremin).

of these compounds: while the hole doped systems are crystallized in T-structure (apical oxygen above in-plane copper), the electron doped systems has T'-structure in which apical oxygen is shifted and appears above in-plane oxygen.

The t–J and Hubbard-like models are widely employed to investigate HTSC compounds. While using these models one, in principle, can catch up qualitatively low-energy physics, the parameters in these models, i.e., the hopping integral t, antiferromagnetic exchange J, Hubbard repulsion U, are usually taken from experimental data. Thus, these parameters do not have a direct microscopical meaning. A more rigorous approach is to write down the multi-band Hamiltonian which includes parameters of the real structure and map this Hamiltonian onto some low-energy model like t–J Hamiltonian. In this case parameters of the real structure can be taken from ab initio calculations or fitted to experimental data.

As a starting model that properly describes electronic structure of the cuprates it is convenient to use 3-band p–d model [6,7] or the multi-band p–d model [8]. While the first one is simpler it lacks for some significant features, namely importance of d_{z^2} orbitals on copper and p_z orbitals on apical oxygen. A non-zero occupancy of d_{z^2} orbitals was pointed out in XAS and EELS experiments which show 1.5–10% occupancy of d_{z^2} orbitals [9,10] and 15% doping dependent occupancy of p_z orbitals [11] in all high-T_c cuprates of p-type. In order to take into account these facts the multi-band p–d model should be used:

$$H_{pd} = \sum_{f,\lambda,\sigma} (\epsilon_\lambda - \mu) n_{f\lambda\sigma} + \sum_{\langle f,g \rangle} \sum_{\lambda,\lambda',\sigma} T_{fg}^{\lambda\lambda'} c_{f\lambda'\sigma}^+ c_{g\lambda'\sigma}$$
$$+ \sum_{f,g,\lambda,\lambda'} \sum_{\sigma_1,\sigma_2,\sigma_3,\sigma_4} V_{fg}^{\lambda\lambda'} c_{f\lambda\sigma_1}^+ c_{f\lambda\sigma_3} c_{g\lambda'\sigma_2}^+ c_{g\lambda'\sigma_4}, \quad (1)$$

where $c_{f\lambda\sigma}$ is the annihilation operator in Wannier representation of the hole at site f (copper or oxygen) at orbital λ with spin σ, $n_{f\lambda\sigma} = c_{f\lambda\sigma}^+ c_{f\lambda\sigma}$. Indices λ run through $d_{x^2-y^2} \equiv d_x$ and $d_{3z^2-r^2} \equiv d_z$ orbitals on copper and p_x, p_y, atomic orbitals on in-plane oxygen site and p_z on the apical oxygen; ϵ_λ denotes one-electron energy of the atomic orbital λ. $T_{fg}^{\lambda\lambda'}$ includes matrix elements of hoppings between copper and oxygen (t_{pd} for hopping

$d_x \leftrightarrow p_x, p_y$; $t_{pd}/\sqrt{3}$ for $d_z \leftrightarrow p_x, p_y$; t'_{pd} for $d_x \leftrightarrow p_z$) and between oxygen and oxygen (t_{pp} for hopping $p_x \leftrightarrow p_y$; t'_{pp} for hopping $p_x, p_y \leftrightarrow p_z$). The Coulomb matrix elements $V_{fg}^{\lambda\lambda'}$ includes intra-atomic Hubbard repulsions of two holes with opposite spins on one copper orbital (U_d) and two different orbitals (V_d) and on one oxygen orbital (U_p, V_p), copper–oxygen (V_{pd}).

For small doping concentrations we assume that the microscopic model parameters do not depend strongly on the doping concentration. The only parameter variable with doping is the electron concentration. In this approach at optimal ($x = 0.15$) and overdoped HTSC where the Fermi liquid properties are known, the conventional band theory is the proper method. In this method the $V_{fg}^{\lambda\lambda'}$ is treated as a perturbation of the single electron band structure. But in the light doping region when strong electron correlations determines the band structure the generalized tight-binding (GTB) calculations with full Hamiltonian (1) should be used. Nevertheless both approaches operates with the same set of the underlying microscopic parameters and the effective parameters like hoppings t, t' are expected to be similar.

For the optimally doped $Nd_{2-x}Ce_xCuO_4$ the Fermi surface topology is described by the tight-binding energy dispersion

$$\epsilon_k = -2t(\cos k_x + \cos k_y) - 4t' \cos k_x \cos k_y + \mu$$
$$(2)$$

taken in accordance with angle-resolved photoemission spectroscopy (ARPES) experiments [12]. The chemical potential μ describes the band filling. Here and in the following we set the lattice constant $a = b$ equal to unity, t is the hopping integral between nearest neighbor sites, and t' is the hopping between next nearest neighbors.

In Fig. 1 the results for ϵ_k of a tight-binding calculation are shown (solid curve). We choose the parameters $t = 0.138$ eV, $t'/t = -0.3$. For comparison, we also show the results with $t = 0.5$ eV and $t'/t = 0$, which is often used to describe the hole-doped superconductors (dashed curve).

Using the resulting ϵ_k and Hubbard Hamiltonian in a spin-fluctuation-induced pairing theory in the framework of the so-called FLEX approxi-
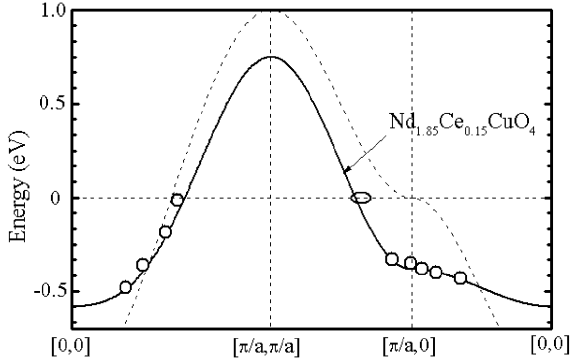
Fig. 1. Results of the energy dispersion ϵ_k of optimally doped NCCO. The solid curve refers to our tight-binding calculation choosing $t = 0.138$ eV and $t'/t = 0.3$. Data (open dots) are taken from [12]. The dashed curve corresponds to using $t = 0.5$ eV and $t'/t = 0$ and is typical for hole-doped cuprates. One immediately sees the important difference: in the case of NCCO the flat band is approximately 0.3 eV below the Fermi level yielding a small density of states, whereas for the hole-doped case the flat band lies very close to it.

mation [13] we find for electron-doped cuprates smaller T_c values due to a flat dispersion ϵ_k around $(\pi, 0)$ well below the Fermi level [14]. This approach yields for electron-doped cuprates, as for hole-doped ones, pure $d_{x^2-y^2}$ symmetry pairing in good agreement with the experiments [15–17]. Furthermore, superconductivity only occurs for a narrow doping range $0.18 > x > 0.13$, because of the onset of antiferromagnetism and, on the other side, due to poorer nesting conditions. We have also analyzed other pairing interactions and find that if the electron–phonon coupling becomes important, for example due to oxygen deficiency, then the s-wave pairing instability competes with $d_{x^2-y^2}$-wave symmetry.

At small doping we have to treat the strong electronic correlations explicitly and thus we use the GTB method [18] that consists of exact diagonalization of the intracell part of p–d Hamiltonian (1) and perturbative treatment of the intercell part. For $La_{2-x}Sr_xCuO_4$ the unit cell is the CuO_6 cluster, and a problem of non-orthogonality of the oxygen molecular orbitals of adjacent cells is solved by an explicit fashion namely by constructing the relevant Wannier functions on a five-orbitals initial basis of the atomic states. In a new symmetric basis an intracell part of the total

Hamiltonian is diagonalized, allowing to classify all possible effective quasiparticle excitations in CuO_2-plane according to a symmetry. Our calculations [19,20] of the quasiparticle dispersion and spectral intensities in the framework of multiband p–d model with use of GTB method are in very good agreement with ARPES data on insulating parent compound $Sr_2CuO_2Cl_2$ [21,22]. The pinning of the Fermi level [23,24] in $La_{2-x}Sr_xCuO_4$ was also obtained according to experiments [5,25]. This pinning appears due to in-gap state–spectral weight of this state is proportional to x and when Fermi level comes to this in-gap band then Fermi level "stacks" there. Experimentally observed [26,27] evolution of Fermi surface from hole-type (centered at (π, π)) to electron-type (centered at $(0, 0)$) with doping in p-type cuprate $La_{2-x}Sr_xCuO_4$ is qualitatively reproduced in this method. Pseudogap feature is obtained as a lowering of the density of states between the in-gap state and the states at the top of the valence band.

Let us now turn to the determination of parameters. According to the difference in atomic structure of LSCO and NCCO the microscopic parameters for NCCO should not have large difference with the parameters in LSCO: the Cu–O and O–O distances in CuO_2 plane are the same, so we keep corresponding parameters t_{pd} and t_{pp} the same. The apical oxygen of LSCO is shifted from the position above copper to the position above the in-plane oxygen, that is why there is no direct hopping from copper to the apical oxygen $t'_{pd} = 0$ in NCCO. The in-plane oxygen–out-plane oxygen distance increases and we change the t'_{pp} parameter from 0.42 eV for LSCO to 0.2 eV in NCCO. Due to smaller optical gap in NCCO we decrease also the charge transfer energy $\epsilon_{p_x} - \epsilon_{d_{x^2-y^2}} = 1.4$ eV in NCCO instead of 1.6 eV in LSCO. All other microscopic parameters are the same and equal to (all values in eV):

$$\epsilon_{d_{x^2-y^2}} = 0.2, \quad \epsilon_{d_{z^2}} = 2, \quad \epsilon_{p_x} = 1.6, \quad \epsilon_{p_z} = 0.45,$$
$$t_{pd} = 1, \quad t_{pp} = 0.56, \quad t'_{pd} = 0, \quad t'_{pp} = 0.2,$$
$$U_d = 9, \quad J_d = 1, \quad U_p = 4, \quad V_{pd} = 1.5.$$

$$(3)$$

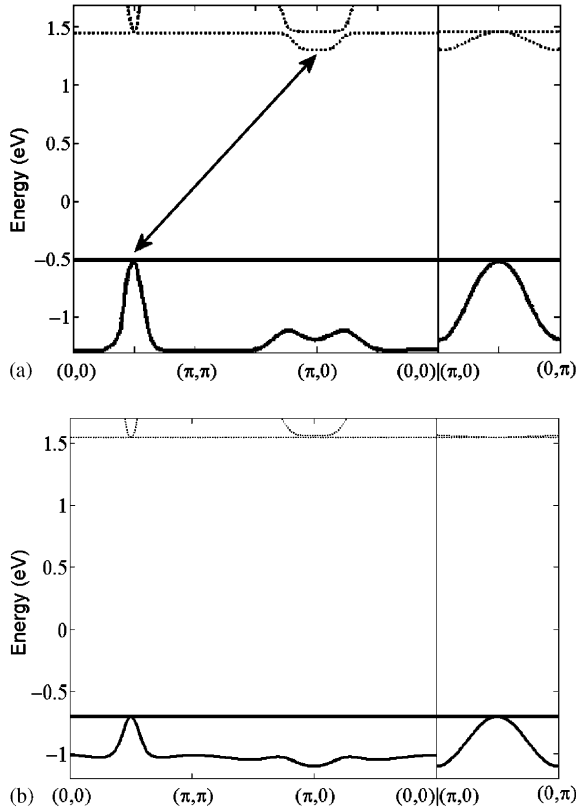This minor and physically well justified changes are sufficient to shift the minimum of the

Fig. 2. GTB method dispersion of the top of the valence band (filled line) and the bottom of the conduction band (dotted line) for $Nd_{2-x}Ce_xCuO_4$ with $x = 0.03$ (a) and for undoped La_2CuO_4 (b). Dispersionless subbands on the top of the valence band and the bottom of the conduction band are the in-gap states which have spectral weight proportional to x. The arrow in (a) marks the indirect insulating gap observed in experiment for NCCO but not for LSCO [4].
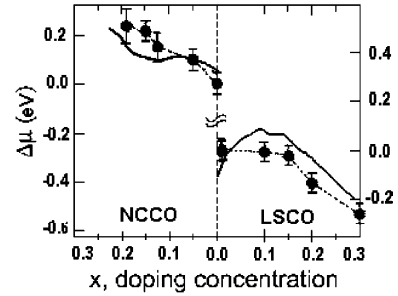

Fig. 3. Dependence of chemical potential shift $\Delta\mu$ on concentration of doping x for NCCO and LSCO. Straight lines are results of GTB calculations [23,24,28], filled circles with error bars are experimental points [5].

conductivity band at $(\pi, 0)$ point below the minimum at $(\pi/2, \pi/2)$ point resulting in the indirect insulator gap found by ARPES measurements (see arrow in Fig. 2(b)). The main contribution to this effect comes from changes in t_{pp} and $\varepsilon_{p_x} - \varepsilon_{d_{x^2-y^2}}$. Contribution from t'_{pd} and t'_{pp} to the bottom of the conduction band is negligible. The localized in-gap state exist in NCCO also for the same reason as in LSCO but its energy appears to be below the bottom of the conductivity band (compare Fig. 2(a) and (b)). Thus, the first doped electron goes into the band state at $(\pi, 0)$ and the chemical potential for the very small concentration merges into the band. At higher x it meets the in-gap state with a

pinning at $0.08 < x < 0.18$ and then μ again moves into the band. The dependence $\mu(x)$ for NCCO is quite asymmetrical to the LSCO and agrees with experimental data [5] (see Fig. 3).

The next step is to formulate the effective model. It is derived by exclusion the intersubband hopping between low (LHB) and upper (UHB) Hubbard subbands via canonical transformations. Using that approach we have obtained an effective Hamiltonian [29] with the asymmetry for n- and p-type systems: for electron-doped systems the usual t–J model takes place while the effective singlet–triplet t–J model is the low-energy model for p-type superconductors. The reason why this asymmetry arises is as follows. There are two low-lying two-hole states: Zhang–Rice-type singlet ^1A_1g and triplet state ^3B_1g. In the 3-band model this triplet state lies above singlet state at energy $\Delta_{TS} = \varepsilon_T - \varepsilon_S = 8J \approx 2$ eV and is unimportant in the low excitation energy limit. Of course, it is a model dependent result and in the more general multiband p–d model Δ_{TS} decreased due to Hund coupling of two holes in $d_{x^2-y^2}$ and d_{z^2} copper orbitals and due to additional hopping t'_{pd} from d_{z^2} copper orbital to p_z orbital of the apical oxygen. For realistic values of parameters in a multi-band p–d model Δ_{TS} is less or equal to 0.5 eV [19]. Thus, we conclude that we cannot drop out singlet–triplet mixing and the complicated structure of the valence band near the binding energies ~0.5 eV. In p-type cuprates it is related to the singlet–triplet transitions. In case of n-type system there is no triplet state in $d^{10}p^6$ configuration and the effective model is much simpler.

Introducing Hubbard X-operators $X_f^{pq} \equiv |p\rangle\langle q|$ at site f we can write down the effective Hamiltonian for n-type cuprates:

$$H_{t-J} = \sum_{f,\sigma} (\varepsilon_1 - \mu) X_f^{\sigma\sigma} + \sum_{\langle f,g \rangle, \sigma} t_{fg}^{00} X_f^{\sigma 0} X_g^{0\sigma}$$
$$+ \sum_{\langle f,g \rangle} J_{fg} \left(\vec{S}_f \vec{S}_g - \frac{1}{4} n_f n_g \right), \qquad (4)$$

where $\vec{S}_f$ denote spin operators and n_f are number of particles operators. The $J_{fg} = 2 \frac{(t_{fg}^{0S})^2}{E_{ct}}$ is the exchange integral. We neglect numerically small triplet correction to the exchange integral $\delta J_{fg} = 2v^2 \frac{(t_{fg}^{ST})^2}{E_{ct}}$. Here E_{ct} is the energy of charge-transfer gap that similar to U in the Hubbard model ($E_{ct} \approx 2$ eV for cuprates).

The relation between parameters in effective Hamiltonian (4) and microscopical parameters of multi-band p–d model is as follows:

$$t_{fg}^{00} = -2t_{pd}\mu_{fg}2uv - 2t_{pp}v_{fg}v^2,$$
$$t_{fg}^{SS} = -2t_{pd}\mu_{fg}2\gamma_x\gamma_b - 2t_{pp}v_{fg}\gamma_b^2,$$
$$t_{fg}^{0S} = 2t_{pd}\mu_{fg}(v\gamma_x - u\gamma_b) + 2t_{pp}v_{fg}v\gamma_b, \qquad (5)$$
$$t_{fg}^{TT} = 2t'_{pd}\lambda_{fg}2\gamma_a\gamma_z + 2t_{pp}v_{fg}\gamma_a^2 - 2t'_{pp}\lambda_{fg}2\gamma_p\gamma_a,$$
$$t_{fg}^{ST} = 2t'_{pd}\xi_{fg}\gamma_z + 2t_{pp}\chi_{fg}\gamma_a - 2t'_{pp}\xi_{fg}\gamma_p,$$

where the upper indices of hopping integrals $(0, S, T)$ correspond to excitations which are accompanied by hopping from site f to g, i.e., in Hamiltonian one has the following terms: $\sum_{\langle f,g \rangle, \sigma} t_{fg}^{MN} X_f^{\sigma M} X_g^{N\sigma}$. Index 0 corresponds to the vacuum state $|0\rangle$, index S corresponds to two-hole singlet state $|S\rangle \equiv |\uparrow,\downarrow\rangle$ of ^1A_1g symmetry and T corresponds to two-hole triplet state $|TM\rangle$ (where $M = +1, 0, -1$) of ^3B_1g symmetry. The factors μ, v, λ, ξ, χ are the coefficients of Wannier transformation made in within our GTB method and u, v, γ_a, γ_b, γ_z, γ_p are the positively defined matrix elements of transformation from representation of annihilation-creation operators to Hubbard X-operators representation.

Now we will proceed to the discussion of the microscopical origin of difference in p- and n-type parameters. In case of electron doping the conduction band is formed by hoppings t_{fg}^{00} and in case of hole doping valence band is formed by t_{fg}^{SS}. The

main difference between p- and n-type systems in terms of microscopical parameters is the vanishing of hoppings to apical oxygen (see Eq. (3)), namely $t'_{pd} = 0$ and lowering of t'_{pp} from 0.42 for p-type systems [19] to 0.2 for n-type systems. This changes significantly the triplet state contribution (t_{fg}^{TT}, t_{fg}^{ST}, see Eq. (5)), but only slightly modifies t_{fg}^{00}, t_{fg}^{SS} and t_{fg}^{0S}. Thus, we safely conclude that there must be no sign difference in hopping parameters for p- and n-type systems. Using set of microscopical parameters (3) we can write down numerical values of essential in n-type systems hopping integral t_{fg}^{00} and exchange integrals J_{fg} (all values in eV): $t_{01}^{00} = 0.407$, $t_{11}^{00} = -0.012$, $t_{02}^{00} = 0.058$, $J_{01} = 0.270$, $J_{11} = 0.001$, $J_{02} = 0.006$.

Next we can compare the parameters obtained in both small and optimally doped regions. In the GTB the band structure is obtained within the Hubbard I approximation and the conductivity band has a filling factor $(1 - x)/2$ multiplied with the t_{fg}^{00} parameter. Using this fact and renormalizing hopping integrals by this multiplier one can write down the corresponding parameters in both approaches (see Table 1).

As one can see the nearest neighbor hopping parameters t are similar indicating that both approaches similarly captures the main contribution to the band structure. The more specific features of the dispersion are described by second nearest neighbor hoppings t'. Comparing these parameters one can see that the signs are the same while the values are significantly different. This issue could be addressed to the restrictions of conventional band theory in the field of strongly correlated electron systems. In case of the t–J model the next nearest neighbor hopping t' contributes mostly to the $(0, \pi)$–$(\pi, 0)$ direction which is the boundary of AFM Brillouin zone, thus there is strong scattering on AFM short-range fluctuations (two points at this direction is connected by AFM nesting vector

Table 1
Comparison of parameters obtained in a tight-binding approximations and in the framework of GTB method

Tight-binding method	GTB method
$t = 0.138$ eV	$t = 0.152$ eV
$t'/t = -0.3$	$t'/t = -0.028$

$\mathbf{Q} = (\pi, \pi)$). The next nearest neighbor hopping t' could be significantly renormalized by this scattering. In conventional band theory the spin fluctuations are treated as a perturbation which may lead to an overestimation of t'. Contrary, in GTB method the strong electron correlations, which is the cause of spin fluctuations and the AFM spin ordering, are included from the very beginning. Hence, in the $(0, \pi)$–$(\pi, 0)$ direction the value of t' is strongly renormalized from the starting point. This leads to reduction of t' in GTB approach compared to bare t' in conventional band theory.

In Refs. [30,31] the doping dependence of chemical potential and electronic states near the Fermi energy in n-type cuprates are investigated by exact diagonalization of t–t'–t''–J model. The ratio t'/t was taken to be -0.34 [32] which is similar to $t'/t = -0.3$ in our conventional band approach. This is not surprising since ratio $t'/t = -0.34$ in Ref. [32] was obtained by fitting to the experimental data for optimally doped NCCO where conventional band approach gives reasonable results.

In conclusion we can say that combining results of two different approaches, namely, conventional band theory and the generalized tight-binding method, we were able to compare parameters of both approaches. We find good agreement between nearest neighbor hopping parameters t. The next nearest neighbor hopping t' has qualitative agreement, but the values of the t'/t ratio are different. This discrepancy is due to an overestimation of t' in conventional band theory. Finally, we argue that there is no microscopical reason for a difference in sign of the hopping parameter t' for p- and n-type systems.

References

[1] G.M. Luke et al., Phys. Rev. B 42 (1990) 7981.
[2] S.J. Hagen, J.I. Peng, et al., Phys. Rev. B 43 (1991) 13606.
[3] H. Takagi, B. Batlog, H.L. Kao, et al., Phys. Rev. Lett. 69 (1992) 2975.
[4] N.P. Armitage, F. Ronning, D.H. Lu, C. Kim, et al., Phys. Rev. Lett. 88 (2002) 257001.
[5] N. Harima, J. Matsuno, A. Fujimori, et al., Phys. Rev. B 64 (2001) 220507(R).
[6] V.J. Emery, Phys. Rev. Lett. 58 (1987) 2794.
[7] C.M. Varma et al., Solid State Commun. 62 (1987) 681.
[8] Y. Gaididei, V. Loktev, Phys. Status Solidi B 147 (1988) 307.
[9] A. Bianconi et al., Phys. Rev. B 38 (1988) 7196.
[10] H. Romberg et al., Phys. Rev. B 41 (1990) 2609.
[11] C.H. Chen et al., Phys. Rev. Lett. 68 (1992) 2543.
[12] D.M. King et al., Phys. Rev. Lett. 70 (1993) 3159.
[13] N.E. Bickers, D.J. Scalapino, S.R. White, Phys. Rev. Lett. 62 (1989) 961.
[14] D. Manske, I. Eremin, K.-H. Bennemann, Phys. Rev. B 62 (2000) 13922.
[15] C.C. Tsuei, J.R. Kirtley, Phys. Rev. Lett. 85 (2000) 182.
[16] J. David Kokales et al., Phys. Rev. Lett. 85 (2000) 3696.
[17] R. Prozorov, R.W. Gianetta, P. Furnier, R.L. Greene, Phys. Rev. Lett. 85 (2000) 3700.
[18] S.G. Ovchinnikov, I.S. Sandalov, Physica C 161 (1989) 607.
[19] V.A. Gavrichkov et al., Phys. Rev. B 64 (2001) 235124.
[20] V.A. Gavrichkov et al., JETP 91 (2000) 369.
[21] B.O. Wells et al., Phys. Rev. Lett. 74 (1995) 964.
[22] C. Duerr et al., Phys. Rev. B 63 (2000) 014505.
[23] A.A. Borisov, V.A. Gavrichkov, S.G. Ovchinnikov, Mod. Phys. Lett. 17 (2003) 479.
[24] A.A. Borisov, V.A. Gavrichkov, S.G. Ovchinnikov, Zh. Eksp. Teor. Fiz. 124 (2003) 862; JETP 97 (2003) 773.
[25] A. Ino, T. Mizokawa, A. Fujimori, et al., Phys. Rev. Lett. 79 (1997) 2101.
[26] A. Ino, C. Kim, M. Nakamura, et al., Phys. Rev. B 65 (2002) 094504.
[27] C. Kim, F. Ronning, A. Damascelli, et al., Phys. Rev. B 65 (2002) 174516.
[28] V.A. Gavrichkov, S.G. Ovchinnikov, JETP (to be published).
[29] M. Korshunov, S. Ovchinnikov, Fiz. Tverd. Tela 43 (2001) 399; Phys. Sol. State 43 (2001) 416.
[30] T. Tohayama, S. Maekawa, Phys. Rev. B 64 (2001) 212505.
[31] T. Tohayama, S. Maekawa, Phys. Rev. B 67 (2003) 092509.
[32] C. Kim et al., Phys. Rev. Lett. 80 (1998) 4245.